AUT Journal of Mechanical Engineering

AUT J. Mech. Eng., 3(2) (2019) 187-196
DOI: 10.22060/ajme.2018.14135.5706

On the Flow and Heat Transfer Analysis of Pipe Conveying Johnson-Segalman Fluid: Analytical Solution and Parametric Studies

M. G. Sobamowo*

Department of Mechanical Engineering, University of Lagos, Lagos, Nigeria

ABSTRACT: In this study, Galerkin's method of weighted residual is used to present simple approximate analytical solutions to flow and heat transfer characteristics in a pipe conveying Johnson-Segalman fluid. The developed approximate analytical solutions are verified with the results in literature. Thereafter, the solutions are used to investigate the effects of the pertinent parameters such as relaxation time parameter, viscosity parameter and Brinkman number on the fluid velocity and the temperature distributions of the pipe flow. From the results, it shows that the fluid velocity and temperature increase with the relaxation time parameter and Brinkman number. It is also established that relaxation time parameter increases with increase in the velocity of the fluid but decreases with increase in the fluid temperature. It is found that the relaxation parameter effect on the velocity distribution are not significant as the viscosity parameter approaches unity and when it is greater than unity. It is hope that the study will provide more physical insight into the flow phenomena.

Review History:

Received: 26 February 2018
Revised: 23 May 2018
Accepted: 17 July 2018
Available Online: 17 July 2018

Keywords:

Heat transfer
Pipe flow
Johnson-Segalman fluid
Analytical solutions
Galerkin's method of weighted residual

1- Introduction

The growing recognitions and the use of various fluids in industrial, biological and engineering applications have shown that many fluids do not obey Newton's law of viscosity. Consequently, in recent times, many research interests have been invoked on the study of the fluids under various conditions. These fluids such as gels, melts and paints, lubricants containing polymer additives, blood, honey, synovial fluid, molten plastics, polymer solutions, tomato sauce, slurries, pastes etc. are often referred to as non-Newtonian fluids [1, 2] as they do not obey Newton's law of viscosity. Also, the limitations and inadequacies of the classical Navier–Stokes equations to effectively describe rheological behaviors of complex fluids used in industrial processing, have led to the formulations of non-Newtonian and non-Navier-Stokes models which could predict the flow of such fluids under various conditions. Therefore, in the past few decades, different types of new models for non-Newtonian fluids such as second-order fluid, third-order fluid, fourth-order fluid, upper-convected Maxwell fluid and Oldroyd-B fluid have been put forward. These classes of non-Newtonian fluids show constant viscosity. However, in reality, at a given temperature and pressure, the viscosity of a non-Newtonian fluid varies with the rate of shear or the previous kinematic history of the fluid [3]. Therefore, it is established that a single constitutive relation cannot be used to describe and predict all non-Newtonian behaviors. Consequently, different rate-type fluids models have been developed to explain the flow behavior of these fluids. Among many fluids of the rate-type models, Johnson–Segalman (J–S) fluid model, a viscoelastic fluid model was developed to allow for non-affine deformations. It is a fluid model that takes into account elastic and memory effects exhibited by most polymeric and biological fluids [4-6]. In recent times, the fluid model has gained a special status among many fluids of the rate type models, as it includes special cases such as the classical Newtonian fluid, Navier-Stokes fluid, Maxwell fluid and Oldroyd-B fluid [6-21]. Unlike most other fluid models, the J–S fluid allows a non-monotone relationship between the shear stress and velocity gradient in simple shear flows for a certain range of material parameters resulting in solutions with discontinuous velocity gradients for planar and cylindrical Poiseuille flow. The model has been used to successfully explain the phenomenon "spurt" which has been used for the description of large increase in the volume to a small increase in the driving pressure gradient [6-21].

Due to the generic nature and the importance of the fluid model in the study of flow behaviors of non-Newtonian fluids, many studies have been carried to describe the non-Newtonian fluid behaviors using the fluid model [6-21]. The evolved non-linear models in the past studies have been solved using different techniques. Although, in some studies, numerical techniques were adopted, the loss of convergence of numerical iterative algorithms for solving the flow of viscoelastic fluids at moderate values of the Deborah number has been a subject of debate over the past decades. Also, Howell [20] pointed out that the numerical simulation of viscoelastic fluid flow becomes more difficult as a physical parameter, the Weissenberg number, increases. Specifically, at a Weissenberg number larger than a critical value, the iterative nonlinear solver fails to converge. Therefore, Hayat et al. [21] applied Homotopy Analysis Method (HAM) to provide approximate solutions to the heat transfer in pipe flow of Johnson-Segalman fluid. The advantages of the

Corresponding author, E-mail: mikegbeminiyi@gmail.com

homotopy analysis method has been pointed out in another work by Hayat [22].
Although, the analysis of flow and heat transfer of Johnson-Segalman fluid have been studied with the aids of difference analytical and numerical methods, many of the approximate analytical methods present complex mathematical analysis that results in analytic expression with large numbers of terms and when such expressions are routinely implemented, they can sometimes lead to erroneous results [23, 24]. Consequently, there is continuous quest for simple yet accurate solution method to solve the non-linear differential equations. In this regard, methods of weighted residual have shown to be promising tools due to their simplicity and high accuracy. The use of Weighted Residual Methods (WRMs) suggests a handy mathematical formulation [25] and they can handle a wide variety of nonlinear Ordinary Differential Equations (ODEs) despite of their orders and natures. Although, there are different types of WRM depending on the weight functions, among all these methods of weighted residual, the Galerkin Method (GM) has shown to be the most accurate [26]. Apart from its high accuracy in prediction, the method avoids the search and the use of variational formulations [27]. Therefore, in this study, Galerkin's method of weighted residual is adopted to present simple approximate analytical solutions to flow and heat transfer characteristics in a pipe conveying Johnson-Segalman fluid. Also, the influences of pertinent parameters such as relaxation time parameter, viscosity parameter and Brinkman number on the fluid velocity and the temperature distributions of the pipe flow are analyzed and discussed.

2- Model Formulation

Consider a steady state pipe flow of incompressible Johnson-Segalman fluid which is induced by pressure gradient in the z-direction (axis of flow) in a circular pipe of radius r_o shown in Fig. 1.

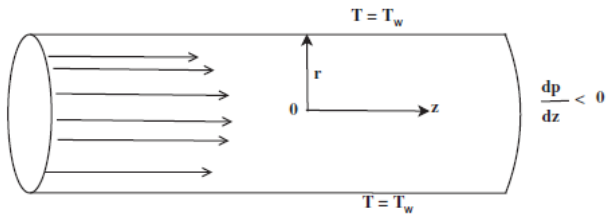

Fig. 1. Schematic of the problem

As the fluid is incompressible, it can undergo only isochoric motions. Therefore, with an appropriate choice of the kernel function and the time constants, the governing equations are

Continuity equation

$$\nabla.\bar{u} = 0 \tag{1}$$

Momentum equation

$$\rho\left(\frac{\partial \bar{u}}{\partial t} + \bar{u}\nabla\bar{u}\right) = \nabla.\sigma \tag{2}$$

Energy equation

$$\sigma\,.\,\Upsilon + k\nabla^2 T = \rho c_p \frac{\partial T}{\partial t} \tag{3}$$

where

$$\sigma = -p\mathrm{I} + \tau \tag{4}$$

$$\tau = 2\mu D + S \tag{5}$$

$$S + \xi\left\{\frac{\partial S}{\partial t} + v\nabla S + S(W - aD) + (W - aD)^t S\right\} = 2\eta D \tag{6}$$

where $\bar{u}$ is the velocity, p is the pressure, ρ is the density, t is time, σ represents the Cauchy stress tensor, $-pI$ is the indeterminate part of the stress due to the constraint of incompressibility, S is an extra stress tensor, T is the temperature, c_p is the specific heat, and k is the thermal conductivity, μ and η are the dynamic viscosities, is ξ the relaxation time and a is the slip parameter. $\boldsymbol{D}$ is a symmetric part of the velocity gradient and $\boldsymbol{W}$ is the skew symmetric part of the velocity gradient, respectively and defined as [6, 11, 21]

$$D = \frac{1}{2}\left(\Upsilon + \Upsilon^t\right) \qquad W = \frac{1}{2}\left(\Upsilon - \Upsilon^t\right) \tag{7}$$

where (t) represents the matrix transpose. It is be noted that this model includes the Oldroyd-B fluid model for a=1. When a=1, μ=0 the Johnson–Segalman fluid model reduces to the Maxwell fluid model, when ξ = 0 the model reduces to the classical Navier–Stokes fluid model and when ξ=0, μ=0 the model reduces to the classical Newtonian fluid model. It should be noted that the bracketed term on the left-hand side of Eq. (6) is an objective time derivative.
The governing equations of motion in cylindrical coordinates give

$$\frac{\partial p}{\partial r} = \frac{1}{r}\frac{d}{dr}\left(rS_{rr}\right) - \frac{S_{\theta\theta}}{r} \tag{8a}$$

$$\frac{\partial p}{\partial \theta} = 0 \tag{8b}$$

$$\frac{\partial p}{\partial z} = \frac{1}{r}\frac{d}{dr}\left(rS_{rz}\right) + \frac{\mu}{r}\frac{d}{dr}\left(r\frac{d\bar{u}}{dr}\right) \tag{8c}$$

$$\begin{aligned}&\left(\frac{d^2T}{dr^2} + \frac{1}{r}\frac{dT}{dr}\right)\left\{1 + \xi\left(1 - a^2\right)\left(\frac{d\bar{u}}{dr}\right)^2\right\}\\ &+ \frac{\mu}{k}\xi\left(1 - a^2\right)\left(\frac{d\bar{u}}{dr}\right)^4 + \frac{(\eta + \mu)}{k}\left(\frac{d\bar{u}}{dr}\right)^2 = 0\end{aligned} \tag{9}$$

where

$$S_{rr}=\frac{-\xi(1-a)\eta\left(\frac{d\bar{u}}{dr}\right)^2}{1+\xi(1-a^2)\left(\frac{d\bar{u}}{dr}\right)^2} \tag{10a}$$

$$S_{rz}=\frac{\eta\frac{d\bar{u}}{dr}}{1+\xi(1-a^2)\left(\frac{d\bar{u}}{dr}\right)^2} \tag{10b}$$

$$S_{\theta\theta}=0 \tag{10c}$$

In the above equations, μ is the variable viscosity, η is the dynamic viscosity, a is the slip parameter ξ is the relaxation time and, r represents the radial direction and S_{rr}, S_{rz}, and $S_{\theta\theta}$ are stresses for the Johnson-Segalman fluid.

It should be noted that while Eqs. (8c) and (9) can be used to find the velocity and temperature distributions in the pipe, Eq. (8a) can be adopted to find the pressure distribution in the pipe. However, our major focus in this work is to find velocity and temperature distributions in the pipe.

From Eqs. (8c) and (10a), we have

$$\frac{\partial p}{\partial z}=\frac{1}{r}\frac{d}{dr}\left\{r\left[\frac{(\eta+\mu)\frac{d\bar{u}}{dr}+\xi\mu(1-a^2)\left(\frac{d\bar{u}}{dr}\right)^3}{1+\xi(1-a^2)\left(\frac{d\bar{u}}{dr}\right)^2}\right]\right\} \tag{11}$$

The boundary condition are given as

$$r=0,\quad \frac{du}{dr}=0,\quad \frac{dT}{dr}=0$$
$$r=r_o,\quad u=0,\quad T=T_w \tag{12}$$

where T_w is the wall temperature.

On non-dimensionalizing Eqs. (9), (11) and (12) using the following dimensionless quantities, where T_m is the wall temperature.

$$R=\frac{r}{r_o},\quad u=\frac{\mu}{\left(\frac{\partial p}{\partial z}\right)r_o^2}\bar{u},\quad \lambda=\frac{\xi\left(1-a^2\right)\left(\frac{\partial p}{\partial z}\right)^2}{\mu^2}r_o^2$$
$$\alpha=\left(1+\frac{\eta}{\mu}\right),\quad \theta=\frac{T-T_w}{T_m-T_w},\quad B_r=\frac{R^4\left(\frac{\partial p}{\partial z}\right)^2}{kT_w\mu} \tag{13}$$

we have

$$\frac{d}{dR}\left\{R\left[\frac{\alpha\frac{du}{dR}+\lambda\left(\frac{du}{dR}\right)^3}{1+\lambda\left(\frac{du}{dR}\right)^2}\right]\right\}-R=0 \tag{14}$$

$$R\frac{d^2\theta}{dR^2}+\frac{1}{R}\frac{d\theta}{dR}+R\lambda\frac{d^2\theta}{dR^2}\left(\frac{du}{dr}\right)^2+\lambda\frac{d\theta}{dR}\left(\frac{du}{dr}\right)^2+R\alpha B_r\left(\frac{d\bar{u}}{dr}\right)^2+R\lambda B_r\left(\frac{du}{dr}\right)^4=0 \tag{15}$$

Eq. (14) can be further simplify after integration of both side with respect to R as

$$2\lambda\left(\frac{du}{dr}\right)^3+2\alpha\frac{du}{dR}-R\lambda\left(\frac{du}{dr}\right)^2-R=0 \tag{16}$$

3- Method of Solution: Galerkin's Method of Weighted Residual

Due to the nonlinearities in Eqs. (15) and (16), Galerkin's method of weighted residual is used. The procedure of the method is described as follows:

Representing the governing equations by

$$L(u)=0\quad in\quad \Omega \tag{17}$$

$$L(\theta)=0\quad in\quad \Omega \tag{18}$$

And

$$u\approx\sum_{i=1}^{N}\varphi_i N_i(R) \tag{19}$$

$$\theta\approx\sum_{i=1}^{N}\phi_i N_i(R) \tag{20}$$

Substitution of the above Eqs. (19) and (20) into Eqs. (17) and (18) results in

$$L(u)\neq 0 \\ =R_e(u)\,(residue) \tag{21}$$

$$L(\theta)\neq 0 \\ =R_e(\theta)\,(residue) \tag{22}$$

The method of weighted residual requires that the parameters $\varphi_1, \varphi_2 \ldots \varphi_n$ and $\phi_1, \phi_2 \ldots \phi_n$ be determined by satisfying

$$\int_\Omega w_{iu}(R)R_e(u)dR \quad \text{with}\quad i=1,2,\ \ldots,\ n \tag{23}$$

$$\int_\Omega w_{i\theta}(R)R_e(\theta)dR \quad \text{with}\quad i=1,2,\ \ldots,\ n \tag{24}$$

where the functions $w_i(R)$ are the n arbitrary weighting functions. There are an infinite number of choices for $w_i(R)$ but four particular functions are most often used.

Since a simple but highly accurate solution is sought, a quadratic trial solution shown in Eqs. (25) and (26) was adopted in this work.

$$u(R)=\beta_o+\beta_1 R+\beta_2 R^2 \tag{25}$$

$$\theta(R)=\psi_o+\psi_1 R+\psi_2 R^2 \tag{26}$$

Ganji [28] pointed out that GM with second degree's trial function converges to result with a good accuracy. Bert [29] had earlier pointed that additional terms should not be necessary in most instances and further refinement should not be necessary.

Thus, the trial function that satisfies the boundary conditions of the momentum and energy Eqs. (16) and (15) could be written as

$$u=-\beta_2(1-R^2) \tag{27}$$

$$\theta=-\psi_2(1-R^2) \tag{28}$$

And the corresponding the weight functions are

$$N_{iu}(R)=1-R^2 \tag{29}$$

$$N_{i\theta}(R)=1-R^2 \tag{30}$$

The Galerkin's formulation of the momentum equation is

$$\int_0^1 N_{iu}(R)\left[2\lambda\left(\frac{du}{dr}\right)^3+2\alpha\frac{du}{dR}-R\lambda\left(\frac{du}{dr}\right)^2-R\right]dR=0 \tag{31}$$

And that of energy equation is

$$\int_0^1 N_{i\theta}(R)\begin{bmatrix} R\dfrac{d^2\theta}{dR^2}+\dfrac{1}{R}\dfrac{d\theta}{dR}+R\lambda\dfrac{d^2\theta}{dR^2}\left(\dfrac{du}{dr}\right)^2 \\ +\lambda\dfrac{d\theta}{dR}\left(\dfrac{du}{dr}\right)^2+R\alpha B_r\left(\dfrac{d\overline{u}}{dr}\right)^2+R\lambda B_r\left(\dfrac{du}{dr}\right)^4\end{bmatrix}dR=0 \tag{32}$$

Substituting the weight function in Eqs. (29) and (30) into Eqs. (31) and (32) respectively, we have;

$$\int_0^1 (1-R^2)\left[2\lambda\left(\frac{du}{dr}\right)^3+2\alpha\frac{du}{dR}-R\lambda\left(\frac{du}{dr}\right)^2-R\right]dR=0 \tag{33}$$

$$\int_0^1 (1-R^2)\begin{bmatrix} R\dfrac{d^2\theta}{dR^2}+\dfrac{1}{R}\dfrac{d\theta}{dR}+R\lambda\dfrac{d^2\theta}{dR^2}\left(\dfrac{du}{dr}\right)^2 \\ +\lambda\dfrac{d\theta}{dR}\left(\dfrac{du}{dr}\right)^2+R\alpha B_r\left(\dfrac{d\overline{u}}{dr}\right)^2+R\lambda B_r\left(\dfrac{du}{dr}\right)^4\end{bmatrix}dR=0 \tag{34}$$

On finding the corresponding terms of Eqs. (15) and (16) from Eqs. (27) and (28) and into Eqs. the same into (34) and (34), yields

$$\beta_2^3-\frac{1}{4}\beta_2^2+\frac{3\alpha}{4\lambda}\beta_2-\frac{3}{16\lambda}=0 \tag{35}$$

$$\psi_2=\frac{-\beta_2^2 B_r\left(2\lambda\beta_2^2+\alpha\right)}{3\left[1+\frac{4}{3}\lambda\beta_2^2\right]} \tag{36}$$

Following the Descartes' rule of polynomial, which states that the number of change of sign in a polynomial is equal to the number of positive roots of the polynomial. The above cubic equation in Eq. (35) changes sign three times. This implies that the cubic equation has three positive roots i.e. all the three roots of the cubic equation are positive. Consequently, it is expected that for all the positive roots of β_2, the dimensionless velocity has negative values and the dimensionless temperature has positive values.

On solving the cubic equation, we have the following roots

$$\beta_{2,1}=2\sqrt{-Q}cos\left(\frac{\vartheta}{3}\right) \tag{37a}$$

$$\beta_{2,2}=2\sqrt{-Q}cos\left[\frac{1}{3}\left(\vartheta+2\pi\right)\right] \tag{37b}$$

$$\beta_{2,3}=2\sqrt{-Q}cos\left[\frac{1}{3}\left(\vartheta+4\pi\right)\right] \tag{37c}$$

where

$$\vartheta=cos^{-1}\left(\frac{-M}{\sqrt{-Q^3}}\right)$$

$$M=\frac{\lambda-54\alpha+162}{1728\lambda}$$

$$Q=\frac{36\alpha-\lambda}{144\lambda}$$

Based on the simulation, the third root $\beta_{2,3}$ gives the most realistic result.

On substituting Eq. (37c) into Eqs. (27) and (28), we have

$$u=-2\sqrt{\frac{\lambda-36\alpha}{144\lambda}}\times$$
$$cos\left\{\frac{1}{3}\left[arccos\left(\frac{54\alpha-\lambda-162}{1728\lambda\sqrt{-\left(\frac{36\alpha-\lambda}{144\lambda}\right)^3}}\right)+4\pi\right]\right\}(1-R^2) \tag{38}$$

$$\theta=\frac{\beta_{2,3}^2 B_r\left(2\lambda\beta_{2,3}^2+\alpha\right)}{3\left[1+\frac{4}{3}\lambda\beta_{2,3}^2\right]}(1-R^2) \tag{39}$$

where

$$\beta_{2,3} = 2\sqrt{\frac{\lambda - 36\alpha}{144\lambda}} \times \cos\left\{\frac{1}{3}\left[\arccos\left(\frac{54\alpha - \lambda - 162}{1728\lambda\sqrt{-\left(\frac{36\alpha - \lambda}{144\lambda}\right)^3}}\right) + 4\pi\right]\right\}$$

The volumetric flow rate, Q_d may be obtained by integrating the flow through a small element $rdrd\phi$ over the cross-sectional area of the pipe

$$Q_d = \int_0^{2\pi}\int_0^{r_o} \bar{u} r dr d\Phi \tag{40}$$

Using the dimensionless parameter

$$Q_{dd} = \frac{\mu Q_d}{\left(\frac{\partial p}{\partial z}\right) r_o^4} \tag{41}$$

The dimensionless volumetric flow rate, Q_{dd} is given as

$$Q_{dd} = \int_0^{2\pi}\int_0^{R} uRdRd\Phi \tag{42}$$

After substituting Eq. (38) and carry out the double integration, we have

$$Q_{dd} = -\frac{\pi}{3}\sqrt{\frac{\lambda - 36\alpha}{144\lambda}} \times \cos\left\{\frac{1}{3}\left[\arccos\left(\frac{54\alpha - \lambda - 162}{1728\lambda\sqrt{-\left(\frac{36\alpha - \lambda}{144\lambda}\right)^3}}\right) + 4\pi\right]\right\} \tag{43}$$

4- Results and Discussion

The numerical results of the developed analytical solutions of fluid velocity and temperature distributions in the half and full cylindrical coordinate systems are presented graphically in Figs. 2 to 27. Effects of pertinent parameters are shown in the figures. Figs. 2 to 7 show the half cylindrical coordinate system of the effects of λ (relaxation time parameter) on the fluid velocity distribution while Figs. 8 to 10 show the velocity profile of half cylindrical coordinate system of the effects of α (viscosity parameter) on the fluid velocity distribution in the pipe. It should be pointed out that while the figures show that velocity increases by increasing λ and α, the effect of λ on the velocity distribution is not significant as α approaches unity and when it is greater than unity as depicted in Figs. 4 to 7.

In order to validate the analytical solutions in this work, the results of the analytical solution of the velocity field using the Galerkin's method of weighted residual are compared with the results of HAM as given by Hayat et al. [20] as shown in Fig. 11. From the graph, it is depicted that the result as presented in this paper agreed well with the results given by

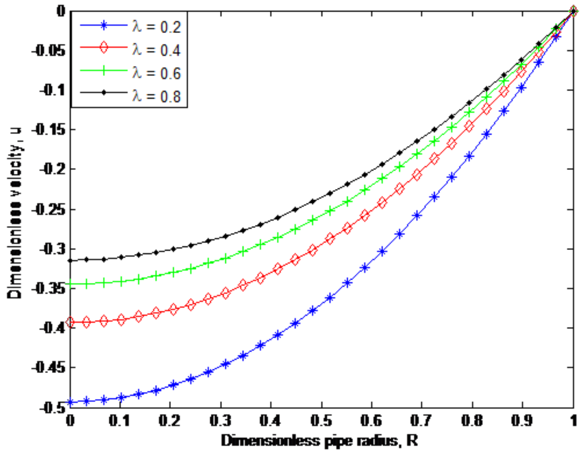

Fig. 2. Effect of λ on the fluid velocity, u when α=0

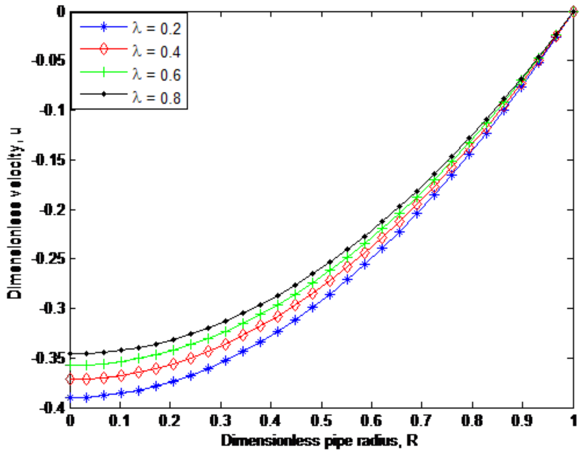

Fig. 3. Effect of λ on the fluid velocity, u when α=0.5

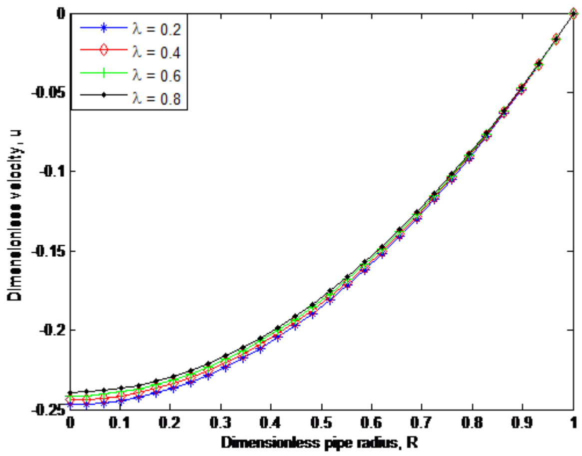

Fig. 4. Effect of λ on the fluid velocity, u when α=0.75

the previous researchers. Therefore, it is established that the use of second degree's trial function in the Galerkin' method of weighted residual converges to good results with high accuracies. This fact had been pointed out earlier studies that additional terms should not be necessary in most instances and further refinement should not be necessary [28, 29].

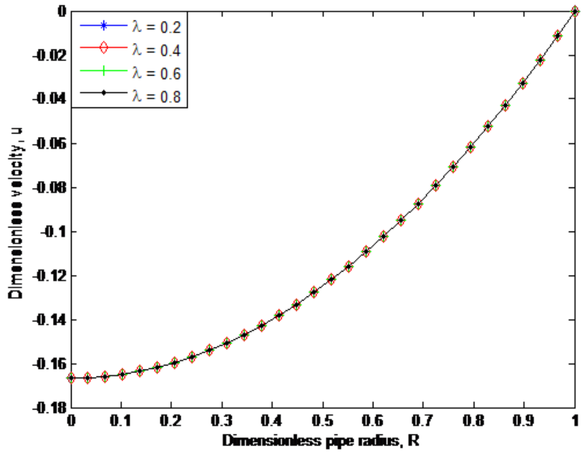

Fig. 5. Effect of λ on the fluid velocity, u when α=1.5

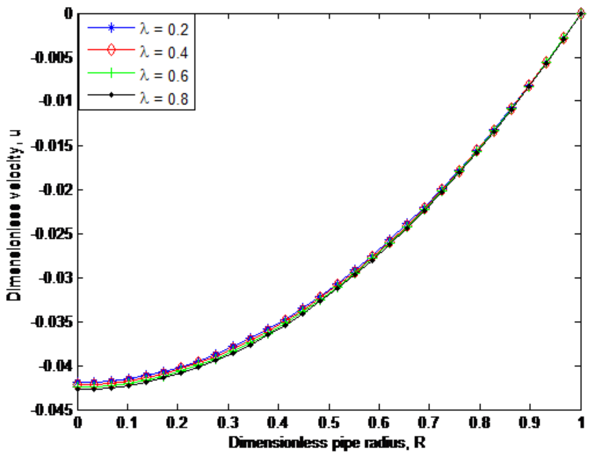

Fig. 6. Effect of λ on the fluid velocity, u when α=2.0

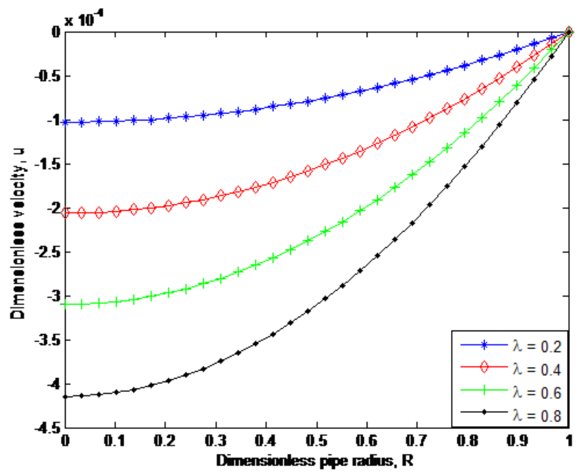

Fig. 7. Effect of λ on the fluid velocity, u when α=3.0

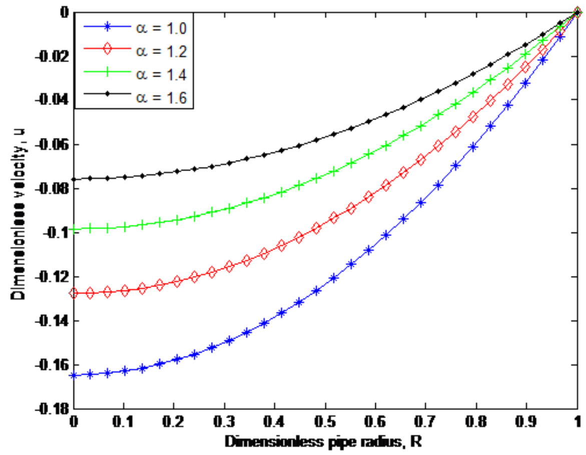

Fig. 8. Effect of α on the fluid velocity, u when λ=0.5

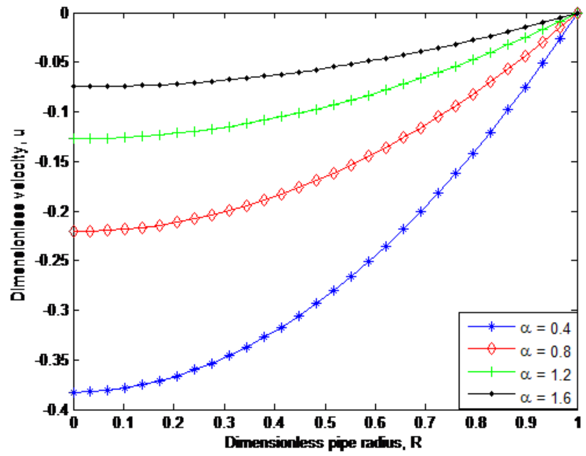

Fig. 9. Effect of α on the fluid velocity, u when λ=0.75

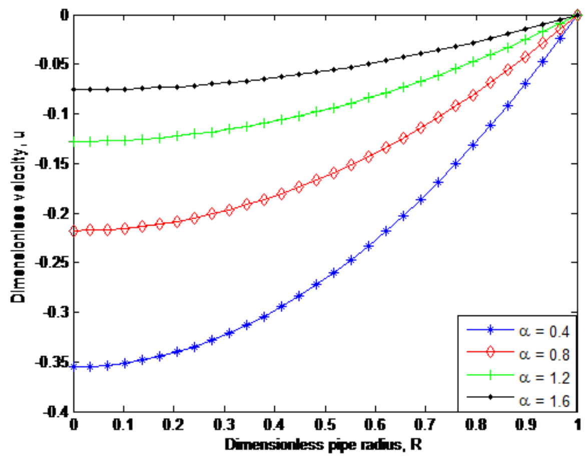

Fig. 10. Effect of α on the fluid velocity, u when λ=1.0

The velocity profile for the full cylindrical coordinate system of the effects of λ and α on the fluid velocity distribution in the pipe are shown in Figs. 12 and 13. Numerically, it could be seen that the velocity is maximum at the center of the pipe with more positive values of λ and α. This is physically true

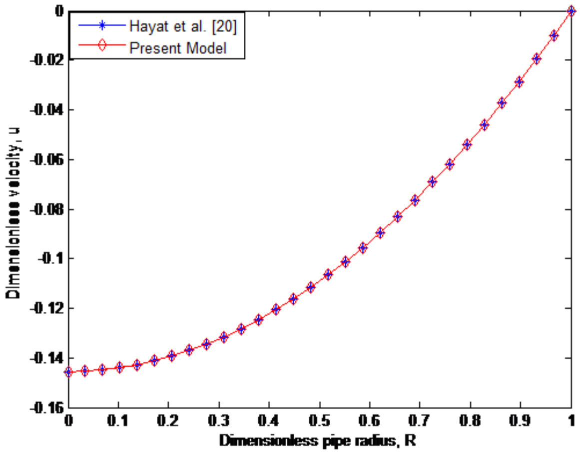

Fig. 11. Comparison of results

because of the axial symmetrical nature of the flow process and the fluid-structure interactions at the pipe walls which lead to the no-slip assumption at the walls. Therefore, the fluid velocity decreases near the walls of the pipe, increases toward the center of the pipe and becomes maximum at the center of the pipe.

Figs. 14 to 21 show the numerical results of the developed analytical solutions of fluid temperature distributions in the half cylindrical coordinate system are presented graphically in Figs. 2 to 27. In the figures, the effects of λ, α, and Brinkman number, B_r on the temperature profiles are presented while Figs. 22 to 27 show the temperature profiles of full cylindrical coordinate system of the effects of λ, α, and B_r on the fluid temperature distribution in the pipe. Although, different studies have been carried out afterwards with different techniques, the results of temperature profiles in the work on the study heat transfer in pipe flow of a Johnson-Segalman fluid as carried out by Hayat et al. [20] show some inconsistencies with the thermal boundary conditions of the developed models. This is because, thermal boundary conditions are not satisfied as shown in their results. Therefore, the present work re-examined the previous analysis with the use of Galerkin's method of weighted residual and present the results accordingly.

It could be seen in the figures that the fluid temperature increases with increase in B_r for different positive values of λ and α as shown in Figs. 14 and 15. The same trends were recorded in Figs. 26 and 27 for the temperature profiles of full cylindrical coordinate system. Figs. 16, 17, 24 and 25 depicts the effects of α on the fluid temperature distributions for different positive values of B_r and λ. The results show that

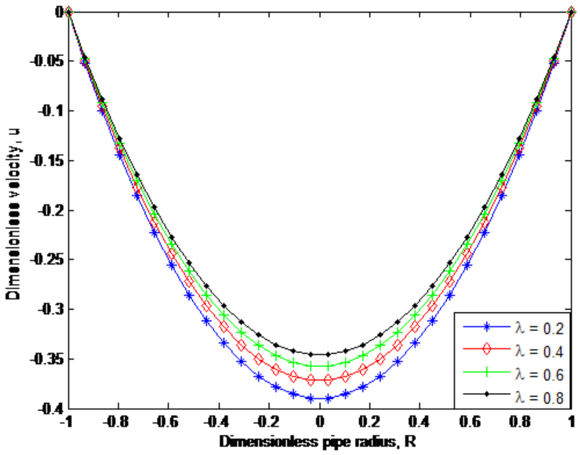

Fig. 12. Effect of λ on the fluid velocity, u when α=0.5

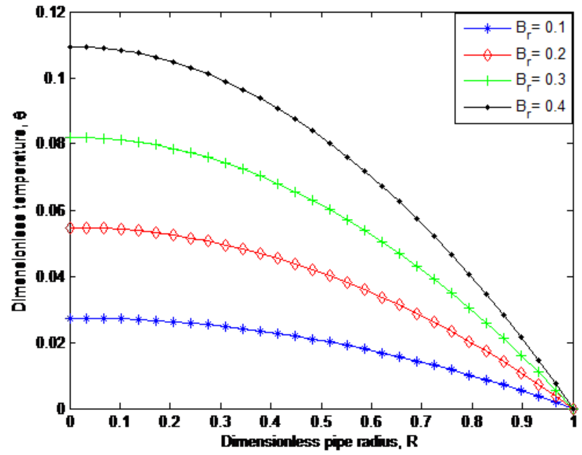

Fig. 14. Effect of B_r on the fluid temperature, λ=0.5, α=0.5

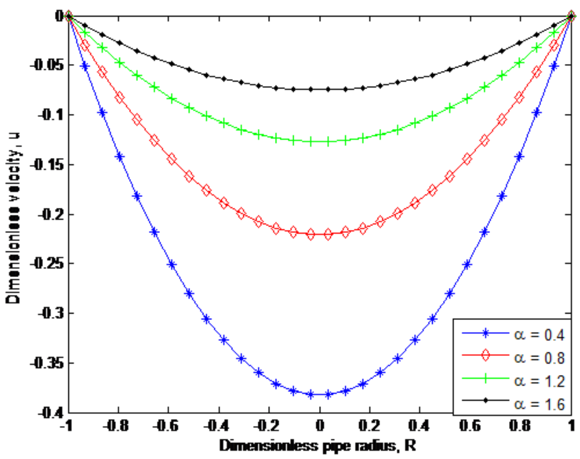

Fig. 13. Effect of α on the fluid velocity, u when λ=0.5

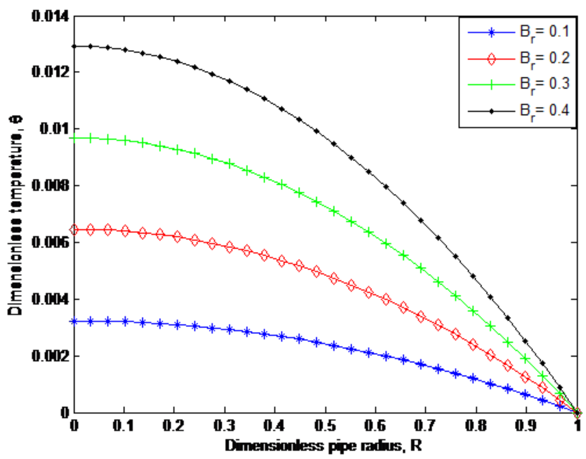

Fig. 15. Effect of B_r on the fluid temperature, λ=0.5, α=1.5

as α increases, the temperature profile of the fluid decreases. This is due to the increase in the fluid viscosity. Also, the effects of λ on the fluid temperature are shown in Figs. 18 to 23. From the figures, it is shown that increase in λ for different positive values of B_r and α lead to increase in fluid temperature. This might be due to increase in the relaxation time of the flow.

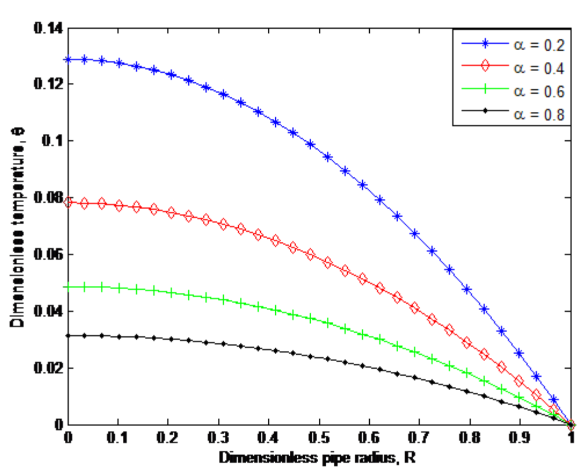

Fig. 16. Effect of α on the fluid temperature, B_r=0.2, λ=0.5

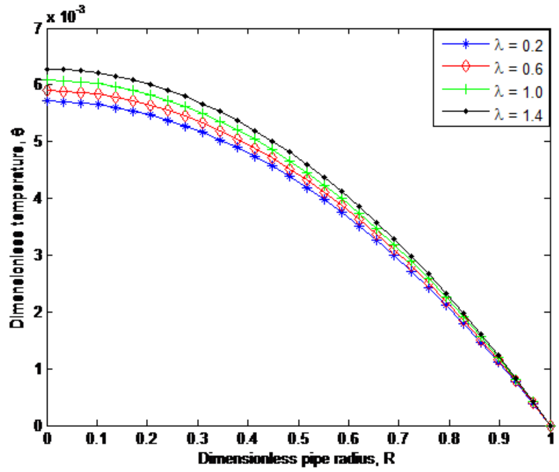

Fig. 19. Effect of λ on the fluid temperature, B_r=0.1, λ=1.2

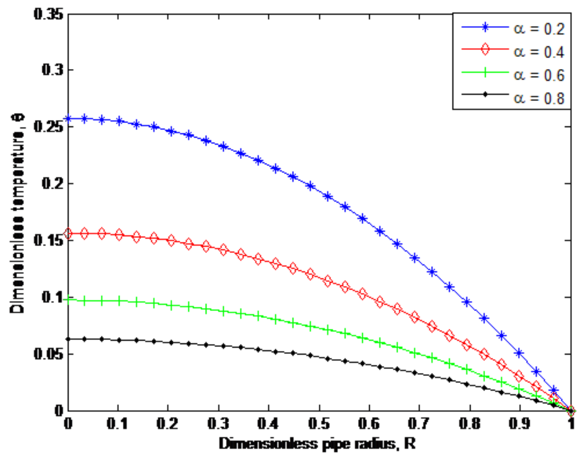

Fig. 17. Effect of α on the fluid temperature, B_r=0.4, λ=0.5

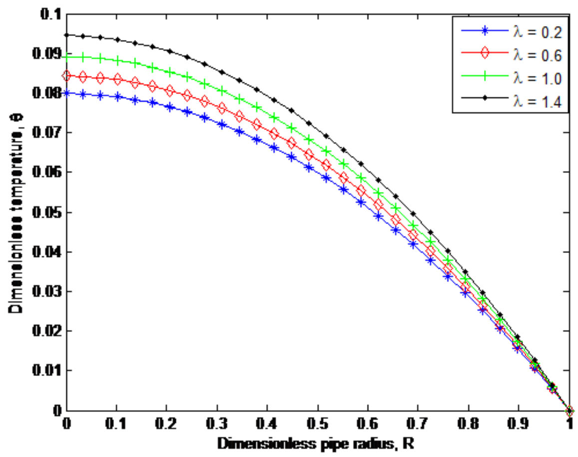

Fig. 20. Effect of λ on the fluid temperature, B_r=0.3, λ=0.5

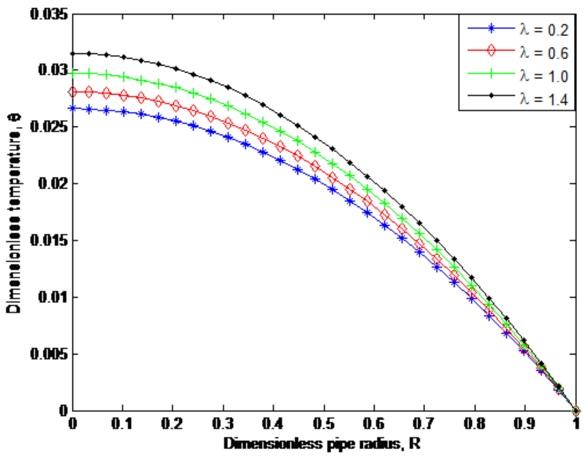

Fig. 18. Effect of λ on the fluid temperature, B_r=0.1, λ=0.5

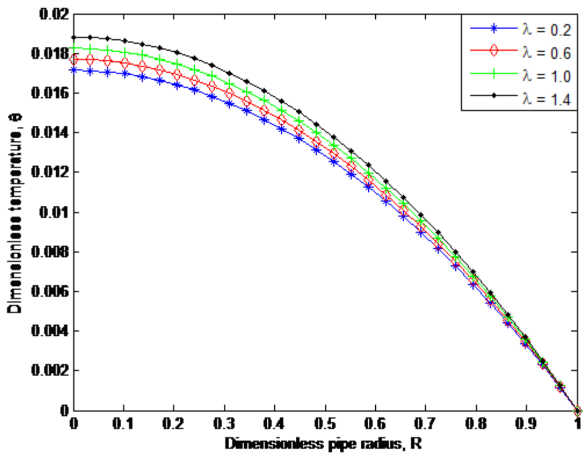

Fig. 21. Effect of λ on the fluid temperature, B_r=0.3, λ=1.2

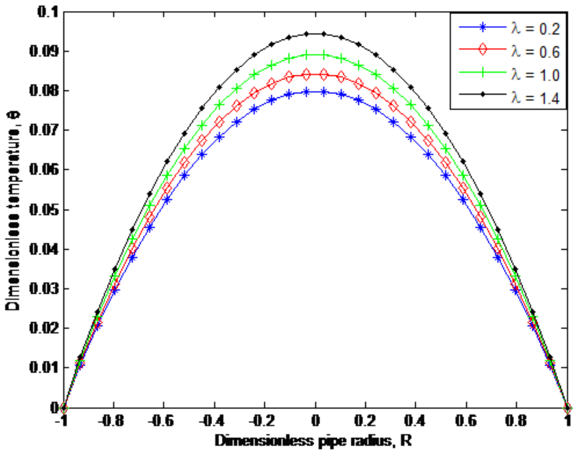

Fig. 22. Effect of λ on the fluid temperature, B_r=0.4, λ=0.5

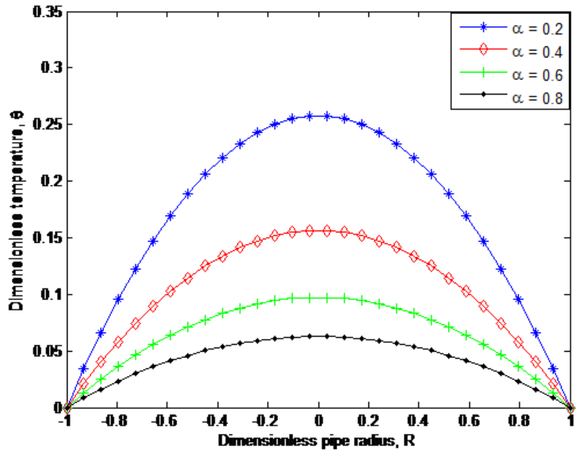

Fig. 25. Effect of λ on the fluid temperature, B_r=0.4, λ=0.5

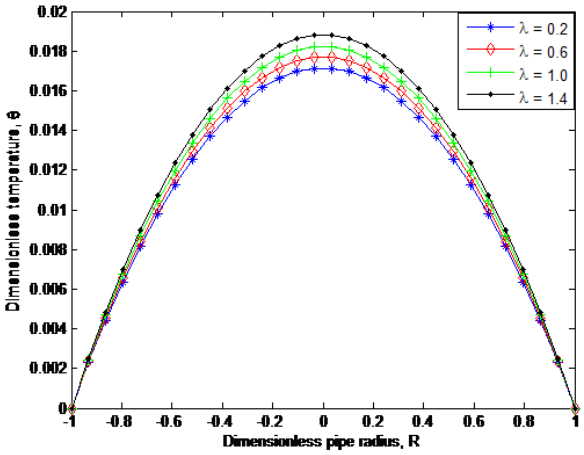

Fig. 23. Effect of λ on the fluid temperature, B_r=0.4, λ=1.2

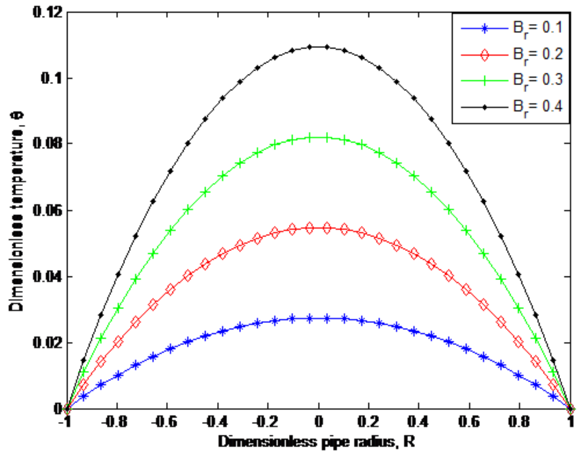

Fig. 26. Effect of λ on the fluid temperature, B_r=0.5, λ=0.5

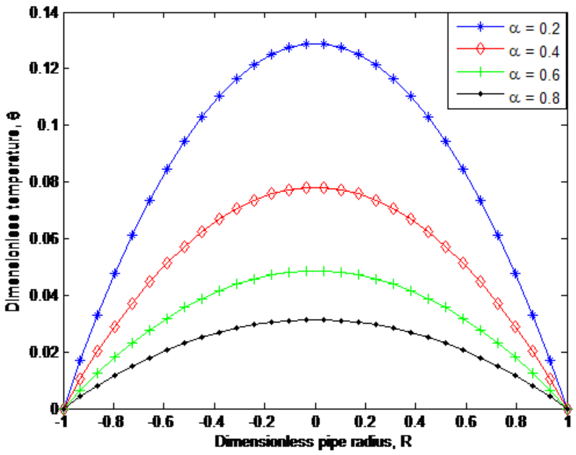

Fig. 24. Effect of λ on the fluid temperature, B_r=0.2, λ=0.5

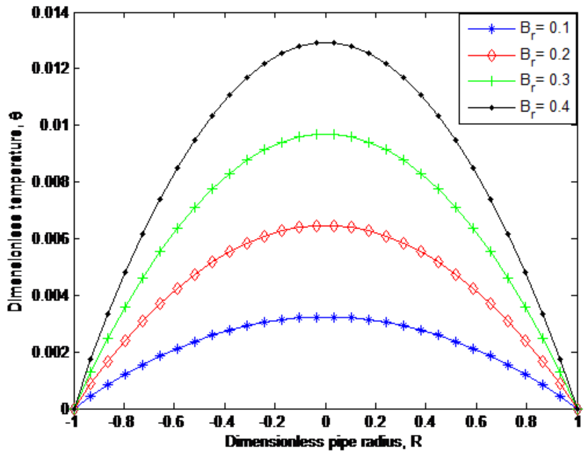

Fig. 27. Effect of λ on the fluid temperature, B_r=1.5, λ=0.5

5- Conclusion

In this paper, steady flow and heat transfer behaviors of Johnson-Segalman in a pipe have been analyzed using Galerkin's method of weighted residual. From the results of the analytical solution developed in the work, it shows that the fluid velocity and temperature increase with the relaxation time parameter and Brinkman number. It was also established that relaxation time parameter increases with increase in the velocity of the fluid but decreases with increase in the fluid temperature. It should be pointed out that the effects of relaxation parameters on the velocity distribution are not significant as the viscosity parameter approaches unity and when it is greater than unity. It is hope that the study will provide more physical insight into the flow phenomena.

References

[1] G. Astarita, G. Marrucci, *Principles of Non-Newtonian Fluid Mechanics*, McGraw-Hill, London, 1974.

[2] R.B. Bird, R.C. Armstrong, O. Hassager, Dynamics of Polymeric Liquids, *Fluid Dynamics*, vol. 1, Wiley, New York, 1987.

[3] X. Qiu, J. Duan, J. Luo, P. N. Kaloni , Y. Liu. Parameter effects on shear stress of Johnson–Segalman fluid in Poiseuille flow. *International Journal of Non-Linear Mechanics*, 55(2010), 140–146.

[4] R.I. Tanner, *Engineering Rheology*, Oxford UniversityPress, Oxford,1992.

[5] M. W. Johnson, D. A. Segalman, Model for viscoelastic fluid behavior which allows non-affine deformation. *J. Non Newton. Fluid Mech.*, 2(1977), 255–270.

[6] M.W. Johnson, D. Segalman, A new model for viscoelastic fluid behavior which allows non-affine deformation, *Journal of Non-Newtonian Fluid Mechanics*, 2(1977), 255–270.

[7] [7] I.J. Rao, K.R. Rajagopal, Some simple flows of a Johnson–Segalman fluid, *Acta Mechanica*, 132(1999), 209–219.

[8] R.W. Kolkka, D.S. Malkus, M.G.Hansen, G.R.Ierley, Spurt phenomena of the Johnson–Segalman fluid and related models, *Journal of Non-Newtonian Fluid Mechanics*, 29(1988), 303–335, 1988.

[9] I.E. Ireka, T. Chinyoka, Non-isothermal flow of a Johnson–Segalman liquid in a lubricated pipe with wall slip, *Journal of Non-Newtonian Fluid Mechanics*, 192(2013), 20–28.

[10] S. Nadeem, N.S. Akbar, Influence of heat and mass transfer on the peristaltic flow of a Johnson–Segalman fluid in a vertical asymmetric channel with induced MHD, *J. Taiwan Inst. Chem. Eng.*, 42(2011), 58–66.

[11] T. Hayat, Y. Wang, A.M. Siddiqui, K. Hutter, Peristaltic motion of a Johnson–Segalman fluid in a planar channel, *Math. Probl. Eng.* 1(2003), 1–23.

[12] T. Hayat, F.M. Mahomed, S. Asghar, Peristaltic flow of a magnetohydrodynamic Johnson–Segalman fluid, *Nonlinear Dynam.*, 40(2005), 375–385.

[13] M. Elshahed, M. Haroun, Peristaltic transport of a Johnson–Segalman fluid under effect of a magnetic field, *Math. Probl. Eng.*, 6(2005), 663–667.

[14] R. W. Kolkka, D.S. Malkus, M.G. Hansen, G.R. IerIy, A.R. Worthing, Spurt phenomenon of the Johnson–Segalman fluid and related models, *J. Non-Newton. Fluid Mech.*, 29(1988), 303–335.

[15] I. J. Rao, K.R. Rajagopal, Some simple flows of a Johnson–Segalman fluid, *Acta Mech.*, 132(1999), 209–219.

[16] M.K. Alam, A.M. Siddiqui , M.T. Rahim, S. Islam Thin-film flow of magnetohydrodynamic (MHD) Johnson–Segalman fluid on vertical surfaces using the Adomian decomposition method. *Applied Mathematics and Computation*, 219(2012), 3956–3974.

[17] S. Hina, T. Hayat, A. Alsaedi Heat and mass transfer effects on the peristaltic flow of Johnson–Segalman fluid in a curved channel with compliant walls, *International Journal of Heat and Mass Transfer*, 55(2012), 3511–3521.

[18] Y. Wang, T. Hayat, K. Hutter, Peristaltic transport of a Johnson–Segalman fluid through a deformable tube, *Theor. Comput. Fluid Dyn*, 21(2007), 369–380.

[19] I. E. Irekaa , T. Chinyokaa Analysis of shear banding phenomena in non-isothermal flow of fluids governed by the diffusive Johnson–Segalman model. *Applied Mathematical Modelling* 40 (2016) 3843–3859.

[20] J. Howell. *Numerical approximation of shear-thinning and Johnson–Segalman viscoelastic fluid flows*. A Dissertation Presented to the Graduate School of Clemson University, 2007.

[21] T. Hayat, Z. Iqbal, M. Sajid, K. Vajravelu. Heat transfer in pipe flow of a Johnson–Segalman fluid, *International Communication in Heat and Mass Transfer*, 35(2008), 1297–1301.

[22] T. Hayat, R. Ellahi, S. Asghar. The influence of variable viscosity and viscous dissipation on the non-Newtonian flow: Analytical solution. *Communication in Nonlinear Science and Numerical Simulation*, 12(2007), 300–313.

[23] A. Fernandez, On some approximate methods for nonlinear models. *Appl Math Comput.*, 215(2009) 168-74.

[24] A. Aziz, and M. N. Bouaziz. A least squares method for a longitudinal fin with temperature dependent internal heat generation and thermal conductivity, *Energy Conversion and Management*, 52(2011), 2876-82.

[25] A. Sadollah, Y. Choi, D. G. Yoo, J. H. Kim, Metaheuristic algorithms for approximate solution to ordinary differential equations of longitudinal fins having various profiles. *Applied Soft Computing*, 33(2015), 360–379.

[26] R. W. Lewis. P. Nithiarasu and K.N. Seetharamu *Fundamental of the Finite Element Method for Heat and Fluid Flow*, John Wiley and Sons. 2004.

[27] M. G. Sobamowo Thermal analysis of longitudinal fin with temperature-dependent properties and internal heat generation using Galerkin's method of weighted residual. *Applied Thermal Engineering*, 99(2016), 1316–1330.

[28] D. D.Ganji. M. Rahgoshay, M. Rahimi and M. Jafari Numerical investigation of fin efficiency and temperature distribution of conductive, convective and radiative straight fins. *IJRRAS*, August 2010

[29] C. W. Bert. An improved approximate method for analyzing steady heat conduction. *Communication in Applied Numerical Methods*, 2(1986), 587-592.

Please cite this article using:

M. G. Sobamowo, On the Flow and Heat Transfer Analysis of Pipe Conveying Johnson-Segalman Fluid: Analytical Solution and Parametric Studies, *AUT J. Mech. Eng.*, 3(2) (2019) 187-196.

DOI: 10.22060/ajme.2018.14135.5706